

See discussions, stats, and author profiles for this publication at: <https://www.researchgate.net/publication/23470532>

# meso -3,5-Bis(trifluoromethyl)phenyl-Substituted Expanded Porphyrins: Synthesis, Characterization, and Optical, Electrochemical, and Photophysical Properties

ARTICLE *in* CHEMISTRY - AN ASIAN JOURNAL · DECEMBER 2008

Impact Factor: 4.59 · DOI: 10.1002/asia.200800229 · Source: PubMed

CITATIONS

13

READS

34

7 AUTHORS, INCLUDING:



**Soonchul Kang**

Kyushu University

31 PUBLICATIONS 568 CITATIONS

SEE PROFILE



**Tomokazu Umeyama**

Kyoto University

97 PUBLICATIONS 3,168 CITATIONS

SEE PROFILE



**Nikolai Tkachenko**

Tampere University of Technology

267 PUBLICATIONS 4,607 CITATIONS

SEE PROFILE



**Helge Lemmetyinen**

Tampere University of Technology

423 PUBLICATIONS 6,456 CITATIONS

SEE PROFILE

# ***meso*-3,5-Bis(trifluoromethyl)phenyl-Substituted Expanded Porphyrins: Synthesis, Characterization, and Optical, Electrochemical, and Photophysical Properties**

Soonchul Kang,<sup>[a]</sup> Hironobu Hayashi,<sup>[a]</sup> Tomokazu Umeyama,<sup>[a]</sup> Yoshihiro Matano,<sup>[a]</sup> Nikolai V. Tkachenko,<sup>\*,[b]</sup> Helge Lemmetyinen,<sup>[b]</sup> and Hiroshi Imahori<sup>\*,[a, c, d]</sup>

**Abstract:** Trifluoroacetic acid-catalyzed condensation of pyrrole with electron-deficient and sterically hindered 3,5-bis(trifluoromethyl)benzaldehyde results in the unexpected production of a series of *meso*-3,5-bis(trifluoromethyl)-phenyl-substituted expanded porphyrins including [22]sapphyrin **2**, *N*-fused [22]pentaphyrin **3**, [26]hexaphyrin **4**, and intact [32]heptaphyrin **5** together

with the conventional 5,10,15,20-tetrakis(3,5-bis(trifluoromethyl)phenyl)porphyrin **1**. These expanded porphyrins are characterized by mass spectrometry, <sup>1</sup>H NMR spectroscopy, UV/

**Keywords:** aromaticity • electrochemistry • macrocycles • photophysics • porphyrinoids

Vis/NIR absorption spectroscopy, and fluorescence spectroscopy. The optical and electrochemical measurements reveal a decrease in the HOMO–LUMO gap with increasing size of the conjugated macrocycles, and in accordance with the trend, the deactivation of the excited singlet state to the ground state is enhanced.

## **Introduction**

Porphyrins contain an extensively conjugated  $\pi$  system, and such a highly delocalized  $\pi$  system is suitable for efficient electron-transfer reactions, because the uptake or release of electrons results in minimal changes of structure and solva-

tion on electron transfer.<sup>[1,2]</sup> Thus, porphyrins have been frequently employed as a component in electron-transfer reactions.<sup>[1,2]</sup> To optimize the electron-transfer properties or to shed light on the electron-transfer mechanism, it is essential to prepare porphyrins with electron-donating or electron-withdrawing groups, which allows control of the electron-transfer reactions. For instance, electron-deficient porphyrins with electron-withdrawing groups have been used as catalysts,<sup>[3]</sup> photosensitizers,<sup>[4]</sup> and building blocks in supra- and super-molecular systems<sup>[5]</sup> and photonic devices.<sup>[6]</sup>


To satisfy the requirement, various electron-withdrawing groups have been attached to the porphyrin ring; specific examples include  $\beta$ - and *meso*-modified porphyrins bearing fluoro, chloro, bromo, cyano, nitro, or perfluoroalkyl groups.<sup>[7–10]</sup> In particular, chemically stable perfluoroalkyl groups have been introduced into the  $\beta$ - or *meso*-positions of the porphyrin ring to alter the electronic structure considerably.<sup>[8–10]</sup> 5,10,15,20-Tetrakis(perfluoroalkyl)porphyrinatozinc(II) possesses HOMO and LUMO levels that are stabilized uniformly by nearly 0.7 V relative to 5,10,15,20-tetraphenylporphyrinatozinc(II).<sup>[9c]</sup> Considering that the widely used 5,10,15,20-tetraphenylporphyrins (TPP) are synthesized from the corresponding aryl aldehyde and pyrrole, it is crucial to establish a general route for the introduction of perfluoroalkyl moieties into the *meso*-aryl groups of porphyrins, which exhibit electron-deficient properties.

[a] S. Kang, H. Hayashi, Dr. T. Umeyama, Prof. Y. Matano, Prof. H. Imahori  
Department of Molecular Engineering  
Graduate School of Engineering  
Kyoto University, Nishikyo-ku, Kyoto 615-8510 (Japan)  
Fax: (+81) 75-383-2571  
E-mail: imahori@scl.kyoto-u.ac.jp

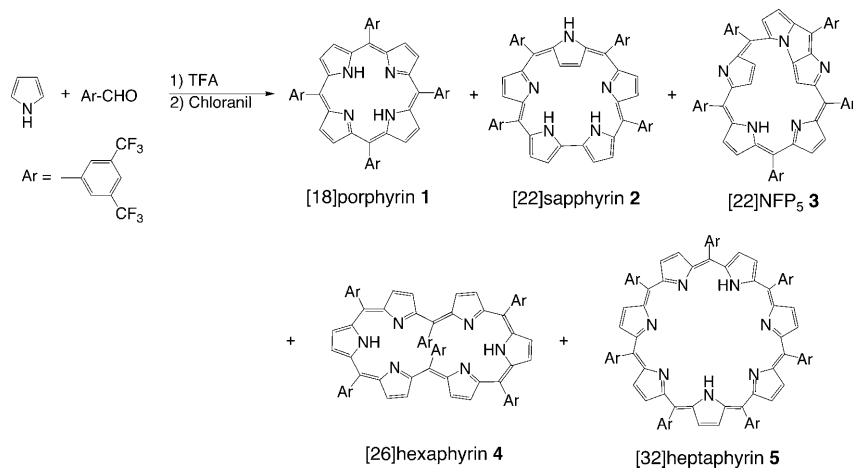
[b] Prof. N. V. Tkachenko, Prof. H. Lemmetyinen  
Institute of Materials Chemistry  
Tampere University of Technology  
P. O. Box 541, Korkeakoulunkatu 8, FIN-33101, Tampere (Finland)  
Fax: (+358) 3-3115-2108  
E-mail: nikolai.tkachenko@tut.fi

[c] Prof. H. Imahori  
Institute for Integrated Cell-Material Sciences (iCeMS)  
Kyoto University, Nishikyo-ku, Kyoto 615-8510 (Japan)

[d] Prof. H. Imahori  
Fukui Institute for Fundamental Chemistry  
Kyoto University, 34-4, Takano-Nishihiraki-cho  
Sakyo-ku, Kyoto 606-8103 (Japan)

 Supporting information for this article is available on the WWW under <http://dx.doi.org/10.1002/asia.200800229>.

During the course of our studies on the synthesis of electron-deficient 5,10,15,20-(3,5-bis(trifluoromethyl)phenyl)porphyrin **1** from 3,5-bis(trifluoromethyl)benzaldehyde and pyrrole under acidic conditions, we accidentally obtained a series of the corresponding expanded porphyrins **2–5** in addition to conventional porphyrin **1** (Scheme 1). The acid-cat-



Scheme 1. Synthesis of a series of *meso*-3,5-bis(trifluoromethyl)phenyl-substituted expanded porphyrins **2–5** and porphyrin **1**.

alyzed one-pot condensation of pyrrole with benzaldehyde to yield *meso*-aryl-substituted expanded porphyrins has been limited to a combination of pyrrole and benzaldehydes, which bear electron-deficient, bulky substituents at both *ortho*-positions.<sup>[11–17]</sup> This unexpected finding has led us to initiate studies on the synthesis and characterization of the expanded porphyrins **2–5**. Herein, we report the structures and optical, electrochemical, and photophysical properties of the expanded porphyrins, which were investigated by using <sup>1</sup>H NMR spectroscopy, UV/visible/near-infrared (NIR) absorption spectroscopy, steady-state fluorescence spectroscopy, cyclic voltammetry, differential pulse voltammetry, fluorescence lifetime measurements, and time-resolved transient absorption spectroscopy. The comprehensive comparison of the expanded porphyrins together with the previously reported analogues and reference porphyrin provides us basic and valuable information on the chemistry of expanded porphyrins, as well as the synthesis of electron-deficient porphyrins.

## Results and Discussion

### Synthesis and Characterization

A solution of 3,5-bis(trifluoromethyl)benzaldehyde and pyrrole (20 mM each) in CH<sub>2</sub>Cl<sub>2</sub> (200 mL) was treated with trifluoroacetic acid (TFA, 4 mmol, 20 mM) for 8 h, followed by oxidation with chloranil (4 mmol). The resultant mixture was separated by chromatography on a silica-gel column with CH<sub>2</sub>Cl<sub>2</sub>/hexane as eluent to afford porphyrin **1** (5%),

sapphyrin **2** (2%), *N*-fused pentaphyrin **3** (1%), hexaphyrin **4** (7%), and heptaphyrin **5** (6%). The molecular structures were characterized by various spectroscopic methods (see Experimental Section). The synthesis of *meso*-aryl-substituted expanded porphyrins from pyrrole and aryl aldehyde has been limited to the acid-catalyzed condensation of pyrrole

with 2,6-disubstituted benzaldehydes, such as 2,3,4,5,6-pentafluorobenzaldehyde, 2,6-difluorobenzaldehyde, 2,4,6-trifluorobenzaldehyde, 2,6-difluorobenzaldehyde, and 4,6-dichloro-2-phenylpyrimidine-5-carbaldehyde.<sup>[18,19]</sup> On the other hand, it

was reported that benzaldehyde, 2-halobenzaldehyde, 2,4-dihalobenzaldehyde, and 2,6-dimethylbenzaldehyde failed to give expanded porphyrins under similar conditions.<sup>[18,19]</sup>

Therefore, to the best of our knowledge, this is the first example of *meso*-aryl-substituted expanded porphyrins with electron-deficient and bulky substituents at both the 3- and 5-positions from one-pot pyrrole-

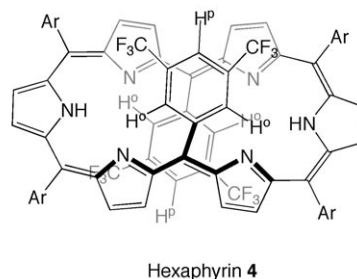
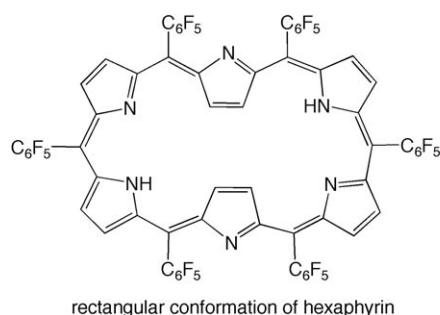
aldehyde condensations. These results suggest that the synthesis of *meso*-aryl-substituted expanded porphyrins requires aryl aldehyde, which bears strong electron-withdrawing substituents rather than the sterically hindered ones at the 2- and 6-positions of the aryl unit. It is noteworthy that the utilization of BF<sub>3</sub>·OEt<sub>2</sub> instead of TFA as a catalyst resulted in the sole production of porphyrin **1** in 18% yield. TFA is a powerful Brønsted-acid catalyst in organic medium and the TFA-catalyzed condensation of pyrrole with aryl aldehyde to yield expanded porphyrins may originate from the “anion template effect”, by which the trifluoroacetate ion plays a crucial templating role, and such effects are rare but are known in the literature.<sup>[20,21]</sup> Additionally, the amount of acid catalyst would affect the TFA-catalyzed condensation.

The <sup>1</sup>H NMR spectra of the sapphyrin **2** in CD<sub>2</sub>Cl<sub>2</sub> show distinct, sharp peaks for all of the protons at low temperatures (Figure S1 in the Supporting Information). These chemical shifts are similar to those of the corresponding protons of previously reported *meso*-aryl-substituted sapphyrins.<sup>[22a]</sup> Grażyński and co-workers<sup>[22]</sup> have reported that the pyrrole ring opposite to the bipyrolic unit in *meso*-aryl sapphyrins is inverted in its free base form on the basis of <sup>1</sup>H NMR chemical shifts observed for the NH proton and the β-pyrrole protons of the inverted ring. In the *meso*-aryl sapphyrin **2** reported here, such a ring inversion is indeed observed (Figure S1 in the Supporting Information). With decreasing temperature from 25 °C to –50 °C, the broad peaks arising from some of the *ortho*-protons gradually sharpen. The <sup>1</sup>H NMR spectrum at –50 °C exhibits two broad singlets at δ = 12.02 and –2.59 ppm occurring from

the outer and inner NH protons. The outer  $\beta$ -CH protons appear at low field as four doublet signals at  $\delta$ =10.26, 9.15, 9.09, and 8.99 ppm, whereas the inner  $\beta$ -CH protons emerge as a singlet at  $\delta$ =−1.31 ppm. These results indicate that there is a strong diatropic ring current in **2** because of the cyclic 22 $\pi$ -electron conjugation.<sup>[23]</sup>

The *N*-fused pentaphyrin **3** revealed a parent ion at  $m/z$ =1445.1620 (calcd for  $C_{62}H_{25}F_{30}N_5$ :  $m/z$ =1445.1631 [ $M$ ]<sup>+</sup>) in its high-resolution FAB (HRFAB) mass spectrum. The <sup>1</sup>H NMR spectrum of **3** (Figure S2 in the Supporting Information) is similar to that of previously reported *meso*-aryl *N*-fused pentaphyrin.<sup>[24]</sup> The <sup>1</sup>H NMR spectrum in CD<sub>2</sub>Cl<sub>2</sub> at −50 °C displays two doublets at  $\delta$ =2.01 and 1.62 ppm, and a singlet at  $\delta$ =−2.40 ppm arising from the inner  $\beta$ -CH protons and a broad signal at  $\delta$ =1.05 ppm occurring from the inner NH proton. The outer  $\beta$ -CH protons appear at low field as four doublet signals at  $\delta$ =9.60, 9.15, 8.61, and 8.46 ppm and as a singlet at  $\delta$ =9.78 ppm. Thus, a maximal difference in the chemical shifts of the inner and outer pyrrolic  $\beta$ -protons ( $\Delta\delta$ =12.18) is notable for *N*-fused pentaphyrin **3**, as for the large  $\Delta\delta$  value (11.57) of **2** arising from the cyclic 22 $\pi$ -electron conjugation. These results indicate that **3** possesses a distinct ring current as a result of the 22 $\pi$ -aromatic-electron network, as described for the *meso*-aryl *N*-fused pentaphyrin<sup>[24]</sup> as well as for the sapphyrins.<sup>[22]</sup>

The hexaphyrin **4** exhibited a parent ion at  $m/z$ =1736.2121 (calcd for  $C_{78}H_{32}F_{36}N_6$  [ $M$ ]<sup>+</sup>:  $m/z$ =1736.2114) in its HRFAB mass spectrum. The <sup>1</sup>H NMR spectra of **4** are



found to be critically temperature dependent. Figure 1 shows the <sup>1</sup>H NMR spectra in CD<sub>2</sub>Cl<sub>2</sub> at various temperatures. At 25 °C all the protons appear in a narrow range of 5–9 ppm accompanied by broad signals:  $\delta$ =8.55 (br), 8.24 (s), 8.12 (d,  $J$ =4.6 Hz), 7.75 (brs), 7.72 (d,  $J$ =1.6 Hz), 7.44 (d,  $J$ =4.6 Hz), 6.18 (s), 5.80 (s). These results differ substantially from the previously reported *meso*-aryl-substituted [26]hexaphyrins(1.1.1.1.1.1.),<sup>[25]</sup> which have planar and rectangular conformations with two inverted pyrroles. In the <sup>1</sup>H NMR spectrum of *meso*-pentafluorophenyl-substituted [26]hexaphyrin(1.1.1.1.1.1.), the inner NH protons and the inner pyrrolic CH-protons appear as a singlet at  $\delta$ =−1.98 ppm and as a doublet at  $\delta$ =−2.43 ppm, respectively, whereas the outer pyrrolic CH protons are observed as two doublets at  $\delta$ =9.11 and 9.44 ppm.<sup>[18a]</sup> In contrast, for the

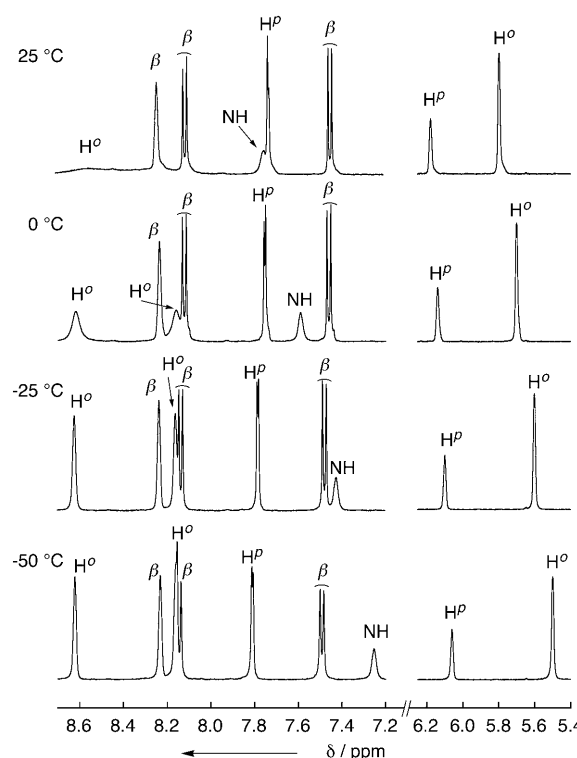


Figure 1. <sup>1</sup>H NMR spectra of hexaphyrin **4** at variable temperatures in CD<sub>2</sub>Cl<sub>2</sub>.

hexaphyrin **4**, there exist no signals at negative  $\delta$  values. The signals at  $\delta$ =7.75 is attributable to the NH protons, as it disappears after shaking with D<sub>2</sub>O. As the temperature decreases from 25 °C to −50 °C, the NH protons gradually shift to the downfield with accompanying line sharpening. Additionally, a new signal appears at  $\delta$ =8.16 with the sharpening of signal at around  $\delta$ =8.55. This is most

likely caused by the gradual conformational fixation of **4** on lowering temperature in the NMR time scale. Although the data were preliminary, the single crystal X-ray diffraction analysis of **4** displayed that two phenyl groups of **4** were found to be located above and below the macrocycle with a planar and rectangular conformation (Figure S3 in the Supporting Information). These results are consistent with the protons emerging at  $\delta$ =6.18 and 5.8, which can be assigned to the *para*- and *ortho*-protons of the two 3,5-bis(trifluoromethyl)phenyl groups arising from the diatropic ring current of the [26]hexaphyrin macrocycle. Recently, Osuka and co-worker reported that the introduction of small aryl substituents, 2-thienyl or 3-thienyl, at both 15- and 30-positions of *meso*-aryl-substituted [26]hexaphyrins(1.1.1.1.1.1.) leads to a stable conformation with all the pyrrole nitrogens pointing

to an inward orientation.<sup>[26]</sup> On the other hand, the hexaphyrin **4** also takes a similar conformation with all the pyrroles pointing to an inward orientation despite the fact that all aryl substituents of **4** are rather bulky. These results suggest the structural diversity of expanded porphyrins with increasing  $\pi$ -conjugation pathway.

The heptaphyrin **5** displayed a parent ion at  $m/z = 207.2602$  (calcd for  $C_{91}H_{39}F_{42}N_7 [M]^+$ :  $m/z = 207.2596$ ) in its HRFAB mass spectrum. The  $^1H$  NMR spectrum of **5** in  $CD_2Cl_2$  at 25 °C exhibits two broad signals at  $\delta = 16.81$  and 11.76 ppm arising from the NH protons, which disappear rapidly upon the addition of  $D_2O$ , seven broad signals at  $\delta = 10.57, 8.96, 7.09, 6.79, 6.09, 5.71$ , and 5.62 caused by the peripheral  $\beta$ -protons, and eight signals at  $\delta = 8.57$ –7.39 occurring from the *ortho*- and *para*-protons of the phenyl groups (Figure S4 in the Supporting Information). The observation suggests a rather rigid, symmetric structure with a nonaromatic  $32\pi$ -electron system. Recently, the concept of Möbius aromaticity that predicts aromatic nature for  $[4n]$  annulenes lying on a twisted Möbius strip has attracted considerable interest from the theoretical and experimental viewpoints.<sup>[27]</sup> Kim, Osuka, and co-workers reported that heptakis(2,6-dichlorophenyl)-substituted [32]heptaphyrin(1.1.1.1.1.1.1) shows several conformers with Möbius-type aromatic character, as revealed by  $^1H$  NMR analysis at low temperature.<sup>[28]</sup> In contrast, the aromaticity of the [32]heptaphyrin **5** is not detected when the  $^1H$  NMR spectra are recorded from 25 °C to –50 °C (Figure S4). This implies that the substituents of *meso*-phenyl groups in heptaphyrins have a large impact on the conformation and aromaticity of heptaphyrins.

The previously reported *meso*-aryl-substituted heptaphyrins are not stable in solution and undergo an *N*-fusion reaction to form *N*-fused heptaphyrins.<sup>[29]</sup> Therefore, the chemistry of heptaphyrin(1.1.1.1.1.1.1) has been left almost unexplored, although the absorption spectra and the X-ray crystal structures of heptaphyrins have been reported. On the other hand, heptaphyrin **5** is stable in solution, because **5** does not have halogen atoms at the 2- and 6-positions of the *meso*-aryl groups, which would be susceptible to intramolecular nucleophilic substitution by the nitrogen atoms of the pyrrole moieties.

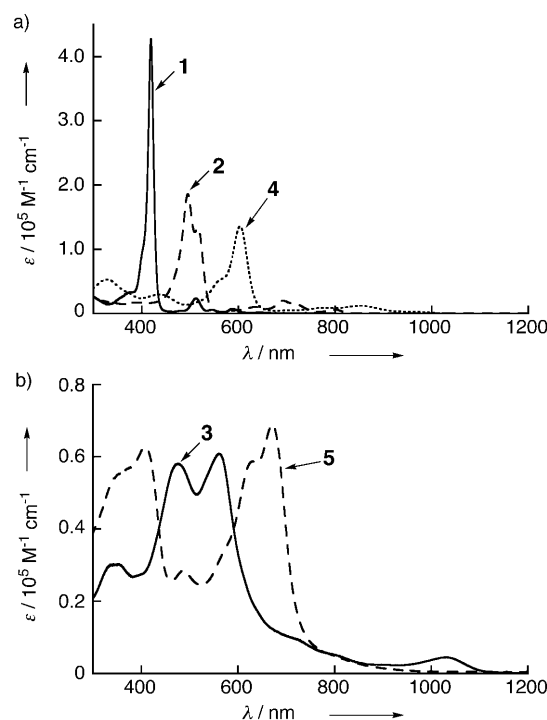


Figure 2. UV/Vis/NIR absorption spectra of a) **1** (—), **2** (---), **4** (....), b) **3** (—), and **5** (---) in toluene.

### Optical Properties

The UV/Vis/NIR absorption spectra of **1–5** were measured in toluene and  $CH_2Cl_2$ . The absorption spectra in toluene are depicted in Figure 2 and the absorption maxima are summarized in Table 1. The absorption spectrum of **1** in toluene reveals an intense Soret band at 419 nm and moderate Q bands at 512, 546, 587, and 644 nm, which are typical characteristics of 5,10,15,20-tetraphenylporphyrins.<sup>[1,2]</sup> The sapphyrin **2** possesses a split Soret-like band at 496 and 517 nm, indicative of polypyrrolic aromatic macrocycles, accompanied by Q bands at 634, 692, 719, and 799 nm.<sup>[30]</sup> The Soret-like band and Q bands of **2** are relatively red-shifted than those of corroles and porphyrins. The aromatic *N*-fused pentaphyrin **3** exhibits a rather broad absorption with four peaks at 345, 477, 560, and 1032 nm. The hexaphyrin **4** displays an intense Soret-like band at 604 nm together with moderate bands at 328 and 438 nm and weak Q-like bands

Table 1. Band maxima of absorption and fluorescence spectra,<sup>[a–c]</sup> Stokes shifts,<sup>[d]</sup> and excited-state lifetimes<sup>[e]</sup> of **1–5**.

	In toluene $\lambda_{abs}^{[a,b]}$ [nm]	$\lambda_{fl}^{[c]}$ [nm]	$\Delta E_{stokes}^{[d]}$ [cm <sup>–1</sup> ]	$\tau^{[e]}$ [ps]	In $CH_2Cl_2$ $\lambda_{abs}^{[a,b]}$ [nm]	$\lambda_{fl}^{[c]}$ [nm]	$\Delta E_{stokes}^{[d]}$ [cm <sup>–1</sup> ]
<b>1</b>	419, <sup>[a]</sup> 644	647	72	10.2 ns <sup>[f]</sup>	417, <sup>[a]</sup> 642 <sup>[b]</sup>	646	96
<b>2</b>	496, <sup>[a]</sup> 517, <sup>[a]</sup> 799 <sup>[b]</sup>	812	200	850 ± 10 <sup>[f]</sup>	492, <sup>[a]</sup> 515, <sup>[a]</sup> 795 <sup>[b]</sup>	808	202
<b>3</b>	477, <sup>[a]</sup> 560, <sup>[a]</sup> 1032 <sup>[b]</sup>	<i>h</i>	–	~0.1 <sup>[g]</sup>	472, <sup>[a]</sup> 560, <sup>[a]</sup> 1022 <sup>[b]</sup>	<i>h</i>	–
<b>4</b>	604, <sup>[a]</sup> 963 <sup>[b]</sup>	998	364	220 ± 20 <sup>[g]</sup>	600, <sup>[a]</sup> 961 <sup>[b]</sup>	994	346
<b>5</b>	628, <sup>[a]</sup> 672 <sup>[a]</sup>	<i>h</i>	–	0.3 <sup>[g]</sup>	626, <sup>[a]</sup> 671 <sup>[a]</sup>	<i>h</i>	–

[a] Absorption wavelength maxima at Soret-like bands. [b] Absorption wavelength maxima at lowest energy Q-like bands. [c] Fluorescence wavelength maxima. [d] Stokes shifts. [e] Excited-state lifetime. [f] Determined by a single photon counting method. [g] Determined by a transient absorption measurement. [h] Not detected.



at 774, 854, and 963 nm. The absorption spectrum of heptaphyrin **5** exhibits split intense bands at 628 and 672 nm as well as at 407 and 486 nm. In general, the Soret-like bands of **1–5** show a systematic red-shift with increasing size of the conjugated macrocycles (Table 1). It is noteworthy that the absorption band at the longest wavelength of **3** reaches into the NIR region (1032 nm), which is considerably longer than those of **4** and **5**. A similar absorption trend is noted for **1–5** in  $\text{CH}_2\text{Cl}_2$  (Table 1). In  $\text{CH}_2\text{Cl}_2$ , we can compare these absorption spectra with the previously reported *meso*-pentafluorophenyl-substituted expanded porphyrins. The Soret band (417 nm) and lowest energy Q band (642 nm) of **1** are red-shifted relative to those of the *meso*-pentafluorophenyl-substituted porphyrin (Soret: 410 nm, Q: 635 nm).<sup>[31]</sup> Such a trend is also seen for *N*-fused pentaphyrin **3**. The Soret-like bands (472, 560 nm) and lowest energy Q-like band (1022 nm) of **3** are red-shifted compared to those of *meso*-pentafluorophenyl-substituted *N*-fused pentaphyrin (Soret: 461, 554 nm, Q: 992 nm).<sup>[24]</sup> These trends may be rationalized by the difference in the electron-withdrawing abilities of *meso*-aryl groups. On the other hand, the hexaphyrin **4** exhibits a Soret-like band at 600 nm, which is red-shifted relative to those of *meso*-pentafluorophenyl-substituted hexaphyrin, whereas the lowest energy Q-like band at 961 nm is blue-shifted in comparison with those of *meso*-pentafluorophenyl-substituted hexaphyrin (1018 nm).<sup>[25b]</sup> Finally, the heptaphyrin **5** reveals split absorption bands at 626 and 671 nm without any low energy bands, while *meso*-pentafluorophenyl-substituted heptaphyrin discloses similar split absorption bands at 598 and 641 nm together with a broad, weak band at 827 nm.<sup>[29a]</sup>

Steady-state fluorescence spectra of **1–5** were measured in toluene and  $\text{CH}_2\text{Cl}_2$ . The expanded porphyrins **3** and **5** did not emit under the present experimental conditions. Figure 3 shows the fluorescence spectra of porphyrin **1** and the expanded porphyrins **2** and **4** in toluene excited at 510 nm, 550 nm, and 605 nm, respectively. The porphyrin **1** displays two emission bands at 647 and 715 nm, which are typical characteristics of 5,10,15,20-tetraphenylporphyrins.<sup>[1,2]</sup> The fluorescence spectrum of **2** in toluene shows two peaks at 812 and 910 nm, while that of **4** reveals intense band at 998 nm together with weak ones at 1106, 1165, and 1210 nm (Figure 3). The Stokes shift increases with increasing size of the macrocycles ( $72\text{ cm}^{-1}$  for **1**,  $200\text{ cm}^{-1}$  for **2**, and  $364\text{ cm}^{-1}$  for **4** in Table 1). The trend may reflect the conformational flexibility with increasing size of the macrocycles. The Stokes shift of **4** is considerably larger than that of *meso*-pentafluorophenyl-substituted [26]hexaphyrin ( $94\text{ cm}^{-1}$ ).<sup>[25b]</sup> which has a rather planar and rectangular conformation with two inverted pyrroles. Similar fluorescence behavior is noted for **1**, **2**, and **4** in  $\text{CH}_2\text{Cl}_2$  (Table 1).

### Electrochemical Properties

The electrochemical properties of the porphyrin **1** and expanded porphyrins **2–5** were evaluated by using cyclic and differential pulsed voltammetry. The electrochemical meas-

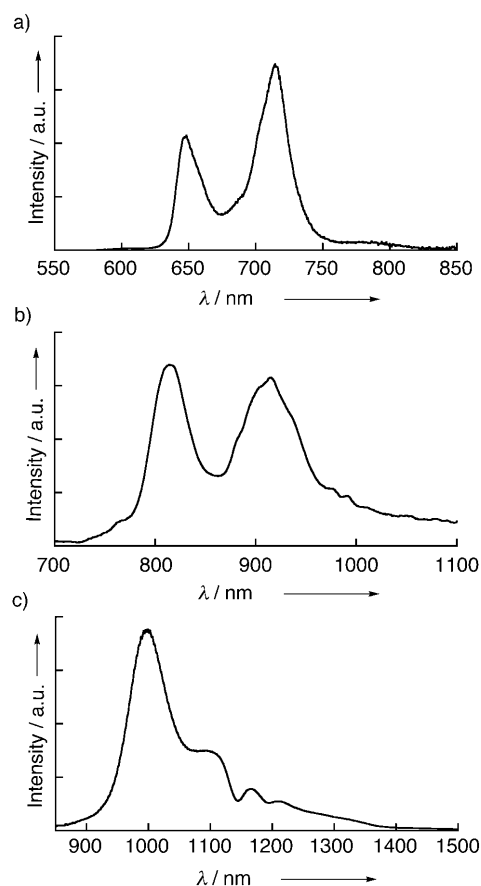


Figure 3. NIR fluorescence spectra of a) **1**, b) **2**, and c) **4** in toluene. Excitation wavelengths were chosen as 510 nm for **1**, 550 nm for **2**, and 605 nm for **4**.

urements were performed in  $\text{CH}_2\text{Cl}_2$  containing 0.1 M tetra-*n*-butylammonium hexafluorophosphate (TBAPF<sub>6</sub>) as a supporting electrolyte. The cyclic voltammograms are shown in Figure 4. For the oxidations, **1**, **2**, and **4** exhibit quasireversible oxidation couples, but **3** and **5** reveal irreversible oxidations. For the reductions, **1**, **3**, **4**, and **5** exhibit quasireversible oxidation couples but not **2**. Some of the redox processes are irreversible and the accurate redox potentials determined by differential pulse voltammetry are listed in Table 2. By comparing the redox potentials of TPP<sup>[32]</sup> and **1**, the porphyrin **1** is more difficult to be oxidized by 0.40 V and easier to be reduced by 0.25 V than TPP. Except **2** and **3**, with increasing size of the macrocycles, the first oxidation potential is shifted to a negative direction, whereas the first reduction potential is shifted to a positive direction. Overall, the difference ( $\Delta_{\text{redox}}$ ) decreases with increasing size of the conjugated macrocycle. This implies a decrease in the electrochemical HOMO–LUMO gap with increasing size of the conjugated macrocycle. The observed red-shifts of the absorption and emission (Table 1) are consistent with this trend. Deviation of **2** and **3** in the trend may result from the direct connection of the two pyrrole units in **2** and the *N*-fused pyrrole moiety of **3**, which would influence the electronic structures of the macrocycles significantly.

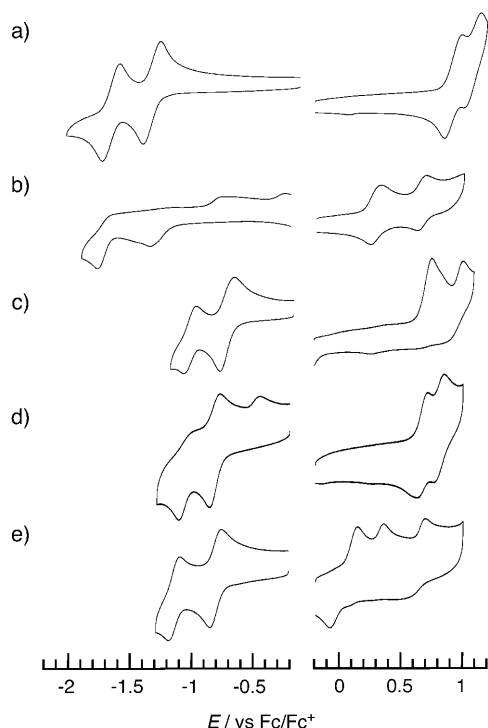


Figure 4. Cyclic voltammograms of a) **1**, b) **2**, c) **3**, d) **4**, and e) **5** in  $\text{CH}_2\text{Cl}_2$  containing 0.1 M TBAPF<sub>6</sub> with a scan rate of 0.2 V s<sup>-1</sup>.

Table 2. Redox potentials (versus Fc/Fc<sup>+</sup>) obtained by differential pulse voltammetry.<sup>[a]</sup>

Compounds	$E_{\text{red}}^2$ [V]	$E_{\text{red}}^1$ [V]	$E_{\text{ox}}^1$ [V]	$E_{\text{ox}}^2$ [V]	$\Delta_{\text{redox}}$ [V] <sup>[b]</sup>
TPP <sup>[c]</sup>	-1.98	-1.67	0.52	0.82	2.19
<b>1</b>	-1.75	-1.42	0.92	1.08	2.34
<b>2</b>	-1.71	-1.29	0.26	0.64	1.55
<b>3</b>	-1.03	-0.74	0.70	0.95	1.44
<b>4</b>	-1.06	-0.82	0.67	0.80	1.49
<b>5</b>	-1.14	-0.80	0.09	0.31	0.89

[a] in  $\text{CH}_2\text{Cl}_2$  using 0.1 M TBAPF<sub>6</sub> as a supporting electrolyte with a sweep rate of 0.01 V s<sup>-1</sup>. [b]  $\Delta_{\text{redox}} = E_{\text{ox}}^1 - E_{\text{red}}^1$ . [c] See Ref. [32].

### Photophysical Properties

An understanding of the excited-state properties of expanded porphyrins is an important prerequisite for their possible applications to materials and biological science and technology. Therefore, to disclose the excited-state dynamics of a series of expanded porphyrins, femto-to-picosecond transient absorption spectra were recorded following photoexcitation at 420 nm in toluene using the pump-probe technique.

For the sapphyrin **2** in toluene, the pump-probe measurements yield two components (Figure 5). The minor short-lived component (0.2 ps) is relatively weak and close to the time resolution of the instrument. This component may correspond to an internal conversion from the higher excited singlet state (generated by 420 nm light) to the lowest singlet excited state. The major decay component (2 ns) shows mainly a bleaching of the ground state absorption, which is similar to conventional porphyrins. The fluorescence lifetime

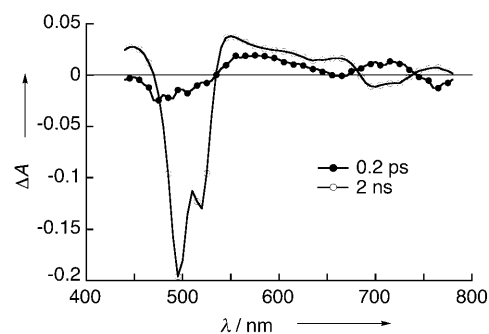


Figure 5. Transient absorption component spectra of **2** in toluene obtained from a global two-exponential fit of the data. Lifetimes of the components are given in the figures.

( $\tau_f$ ) of **2** in toluene was measured with the time-correlated single photon counting apparatus by using an excitation at 650 nm. The fluorescence decay was monitored at 810 nm. The fluorescence decay is mono-exponential with a lifetime of 850 ps (Figure S4 and Table 1). This is a more reliable value for the lifetime of the singlet excited state of **2** than that estimated from the pump-probe measurements (2 ns), as the total time-scanning range of the pump-probe instrument is 1 ns, and most of the molecules in the singlet excited state relax to the triplet excited state, which is also characterized by bleaching of the ground state absorption and is not spectrally resolved on this time scale. The excited-state dynamics of  $\beta$ -alkyl-substituted sapphyrin have already been reported.<sup>[33]</sup> The fluorescence lifetime of 3,8,12,13,17,22-hexaethyl-2,7,18,23-tetramethylsapphyrin is 4.7 ns in  $\text{CH}_2\text{Cl}_2$ ,<sup>[33]</sup> which is approximately 6 times longer than that of **2**. The reason for the shorter lifetime of **2** may arise from the difference in molecular conformations, where all the nitrogens are oriented inward in the case of the  $\beta$ -alkyl-substituted sapphyrin, whereas **2** undergoes a dramatic 180° flip of the inverted pyrrole ring (see earlier).

For the pump-probe experiments of the *N*-fused pentaphyrin **3**, three-exponential fitting gives rise to a reasonably small mean-square-deviation value (Figure 6a). The fast component (0.13 ps) is strong but too short to present a reliable differential spectrum corresponding to the first reaction of the excited pentaphyrin. The following decay can be modeled by two time-resolved components with time constants of 2.2 and 14 ps. It is interesting to note that the transient spectra repeat the vibrational structure of the ground state absorption (typical for photo bleaching) following excitation, but at longer delay times, the picture is changed. Assuming roughly 30 % excitation efficiency, one can calculate the absorption spectrum at 1 ps delay time (Figure 6b). The spectrum at 1 ps resembles the ground state absorption but shows only one maximum. It seems that the *N*-fused pentaphyrin **3** relaxes quickly (100–200 fs) to a state similar to the ground state but with a disturbed conformation (i.e., a non-relaxed vibrational subsystem).

The fluorescence lifetime ( $\tau_f$ ) of **4** in toluene was measured by an up-conversion technique for emission decay measurements in the NIR region by using an excitation at

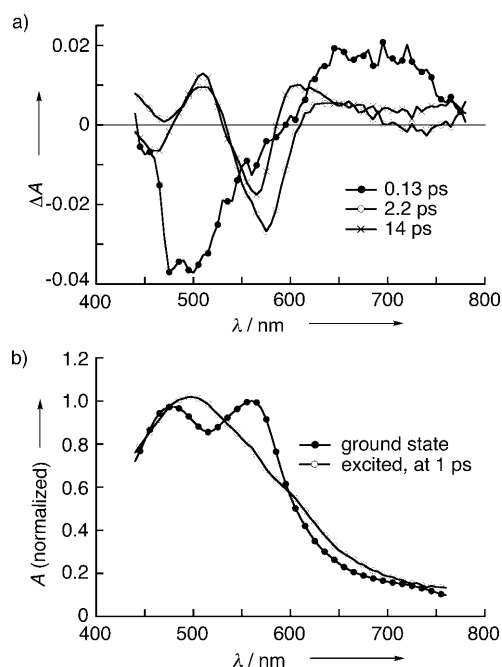


Figure 6. Time-resolved spectroscopy for **3** in toluene: a) Transient absorption component spectra obtained from a global three-exponential fit of the data. Lifetimes of the components are given in the figures. b) Normalized transient absorption spectrum of **3** measured at 1 ps delay time after excitation at 420 nm and ground state absorption spectrum of **3** for comparison.

410 nm. However, **4** was not stable under the excitation beam of the femtosecond laser (average excitation power: ~10 mW, excitation pulse width: ~50 fs) and degraded significantly during the measurements. Hence, we employed the pump-probe measurements to determine the lifetime of the singlet excited state of **4**. Transient absorptions of the hexaphyrin **4** decay almost mono-exponentially with practically no signal in the near infrared part of the spectrum (Figure 7a). The fast component ( $\tau=4.6$  ps) has a minor contribution only, and the main decay component ( $\tau=220$  ps) shows a bleaching of the ground state band at 600 nm and formation of a broad absorption in the visible part of the spectrum. The longer excited singlet state lifetime of **4** ( $\tau=220$  ps) relative to *meso*-hexakis(pentafluorophenyl)[26]hexaphyrin ( $\tau=98$  ps)<sup>[25b]</sup> is attributable to the structural difference between these molecules (see earlier). The spectrum of the 220 ps component is most probably the differential spectrum of the singlet excited state. Assuming 30% excitation efficiency, the absorption spectrum of the singlet excited state can be calculated (Figure 7b).

As described in the <sup>1</sup>H NMR studies, the previously reported normal heptaphyrin(1.1.1.1.1.1.1), *meso*-heptakis(pentafluorophenyl)[32]heptaphyrin,<sup>[29a]</sup> is thermally unstable. It undergoes an *N*-fusion reaction to form singly-*N*-fused heptaphyrin just upon standing in solution. Accordingly, the excited-state dynamics of heptaphyrins have been examined for the first time. For the heptaphyrin **5**, a three-exponential fitting yields a reasonably small mean-square-devi-

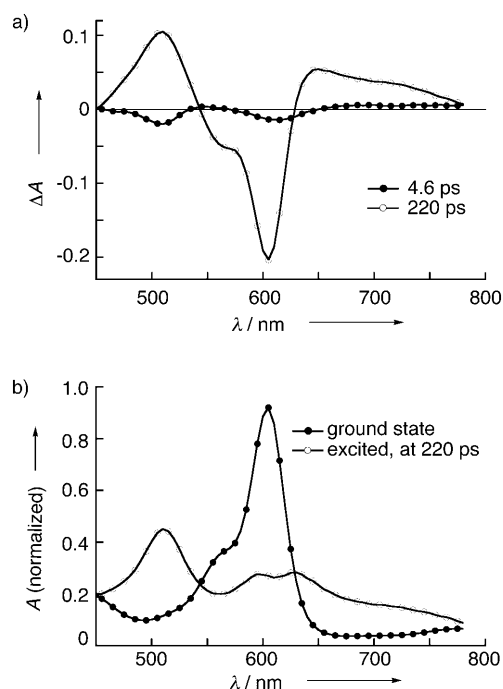


Figure 7. Time-resolved spectroscopy for **4** in toluene: a) Transient absorption component spectra obtained from a global two-exponential fit of the data. Lifetimes of the components are given in the figures. b) Normalized transient absorption spectrum of **4** measured at 220 ps delay time after excitation at 420 nm and ground state absorption spectrum of **4** for comparison.

ation value (Figure 8a). The dominating component is the fast component (0.3 ps), but the 4.6 and 42 ps components are clearly seen at longer delay times, and can be observed separately at some wavelengths. At a 1 ps delay time, the differential spectrum of the sample is the sum of the 4.6 and 42 ps components (cross line in Figure 8b). After 4.6 ps relaxation, the spectrum is changed to that of the longest-lived component ( $\tau=42$  ps). It seems that the electronically excited state of heptaphyrin **5** has a very short lifetime ( $\tau=0.3$  ps) and relaxes to the ground state with a somewhat different configuration or conformation. This “conformationally disturbed” ground state relaxes to the “normal” ground state in two steps with time constants of 4.6 ps and 42 ps, as schematically illustrated in Figure 9.

## Conclusions

In this paper, we have described the synthesis of a series of *meso*-3,5-bis(trifluoromethyl)phenyl-substituted expanded porphyrins in addition to 5,10,15,20-tetrakis(3,5-bis(trifluoromethyl)phenyl)porphyrin. This TFA-catalyzed condensation route is the first example of a one-pot pyrrole-aldehyde condensation to a series of *meso*-aryl substituted expanded porphyrins without bulky, electron-deficient substituents both at the 2- and 6-positions of the aryl aldehyde. The spectral, electrochemical, and excited state studies disclosed various interesting aspects of expanded porphyrins. The optical



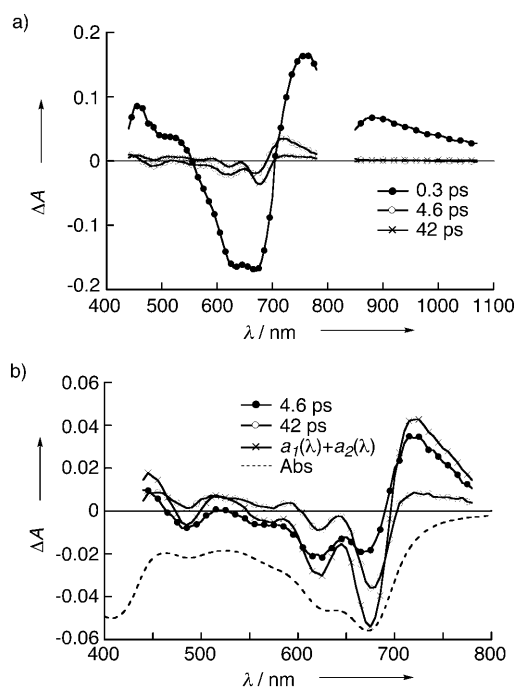


Figure 8. a) Transient absorption component spectra of **5** in toluene obtained from a global three-exponential fit of the data. Lifetimes of the components are given in the figures. b) Transient absorption component spectra of **5** in toluene together with the spectrum obtained by adding the 4.6 and 42 ps components.

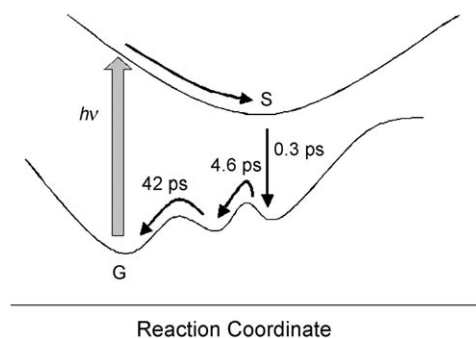


Figure 9. Schematic representation of the potential energy surface and the relaxation pathway for heptaphyrin **5**.

and electrochemical measurements revealed a decrease in the HOMO–LUMO gap with the increasing size of the conjugated macrocycles. In accordance with the trend, deactivation of the excited singlet state to the ground state was enhanced with increasing size of the conjugated macrocycles. It is noteworthy that the thermally stable heptaphyrin shows the unusual nonradiative decay path from the excited singlet state to the ground state. Finally, with the availability of the excellent synthetic methodology for expanded porphyrins, we hope to explore their rich and fascinating chemistry in the future.

## Experimental Section

### General Procedure

Melting points were recorded on a Yanagimoto micro-melting point apparatus and are not corrected.  $^1\text{H}$  NMR spectra were measured on a JEOL EX-270 (270 MHz) or a JEOL EX-400 (400 MHz). High-resolution FAB (HRFAB) mass spectra were recorded on a JEOL JMS-HX110 A spectrometer using 3-nitrobenzyl alcohol. Electrochemical measurements were performed on a CH Instruments model 660 A electrochemical workstation using a glassy carbon working electrode, a platinum wire counter electrode, and an  $\text{Ag}/\text{Ag}^+$  [ $0.01\text{ M AgNO}_3$ ,  $0.1\text{ M nBu}_4\text{NPF}_6$  (acetonitrile)] reference electrode. The potentials were calibrated with ferrocenium/ferrocene [ $E_{\text{mid}} = +0.20\text{ V vs Ag}/\text{Ag}^+$ ]. UV/visible/near IR absorption spectra were recorded by using a Lambda 900 spectrophotometer (Perkin–Elmer, USA). NIR photoluminescence spectra were recorded by using a SHIMADZU NIR-PL System.

### Time-Resolved Spectroscopy Measurements

The time-correlated single photon counting method was used to study emission decays in pico- to nanosecond time domain in the visible part of the spectrum. The samples were excited either at 405 nm or 650 nm by LDH-P-C-405B or LDH-P-650 laser diodes (PicoQuant GmbH), respectively. The emission was detected by a micro-channel photomultiplier (R3809U-50, Hamamatsu Inc.) coupled with a monochromator. The signals were processed by PicoHarp 300 electronic module (PicoQuant GmbH). Typical time resolution of the instrument was 80 ps (FWHM). Transient absorption and fast emission decays were measured by pump-probe and up-conversion experiments, respectively, as described elsewhere.<sup>[34]</sup> In brief, the excitation wavelength was 420 nm (second harmonic of Ti:sapphire laser). A white-light continuum was used as the probe in pump-probe measurements, and the transient spectra were recorded by a cooled CCD detector coupled with a monochromator. The transient spectra were measured in the 450–1100 nm wavelength range. The time resolution was roughly 200 fs (FWHM) for both instruments, and the maximum time scan range was 1 ns.

### Materials

All solvents and chemicals were of reagent-grade quality, obtained commercially, and used without further purification unless otherwise noted. Thin-layer chromatography (TLC) and flash column chromatography were performed with 25 DC-Alufolien Aluminiumoxid 60 F254 Neutral (Merck), and Silica gel 60N (Kanto Chemicals), respectively.

### Preparation of meso-3,5-Bis(trifluoromethyl)phenyl-Substituted Expanded Porphyrins

A solution of 3,5-bis(trifluoromethyl)benzaldehyde (0.73 g, 4 mmol) and pyrrole (0.28 mL, 4 mmol) in  $\text{CH}_2\text{Cl}_2$  (200 mL) was placed in a 300 mL round-bottom flask under nitrogen. To the solution, TFA (0.31 mL, 4 mmol) was added, and the resulting solution was stirred for 8 h. After adding chloranil (0.98 g, 4 mmol), the solution was stirred for 3 h, then passed through a short alumina column to remove the tar. The reaction mixture was then separated by silica-gel column chromatography. By using 10%  $\text{CH}_2\text{Cl}_2$  in hexane, five different colored fractions, that is, green (heptaphyrin), violet (porphyrin), blue (hexaphyrin), yellow (sapphyrin), red (*N*-fused pentaphyrin) ones, were obtained. Each fraction was concentrated, and reprecipitated from  $\text{CH}_2\text{Cl}_2/\text{MeOH}$  to afford porphyrin **1** (5%), sapphyrin **2** (2%), *N*-fused pentaphyrin **3** (1%), hexaphyrin **4** (7%), and heptaphyrin **5** (6%). Synthesis and characterization of porphyrin **1** have already been reported.<sup>[35]</sup>

**[22]Sapphyrin 2:** Yellow solid (20 mg, 2%); m.p.:  $>300^\circ\text{C}$ ; UV/Vis (toluene):  $\lambda_{\text{max}}$  ( $\epsilon$ ) = 317 (20000), 389 (17000), 496 (190000), 517 (130000), 634 (10000), 692 (20000), 719 (15000), 799 nm ( $6100\text{ M}^{-1}\text{cm}^{-1}$ );  $^1\text{H}$  NMR (400 MHz,  $\text{CD}_2\text{Cl}_2$ ,  $-50^\circ\text{C}$ ):  $\delta$  = 12.02 (s, 1H; NH), 10.26 (d,  $J$  = 4.4 Hz, 2H;  $\beta$ -H), 10.06 (s, 2H; *o*-H), 9.15 (d,  $J$  = 4.4 Hz, 2H;  $\beta$ -H), 9.09 (d,  $J$  = 4.4 Hz, 2H;  $\beta$ -H), 8.99 (d,  $J$  = 4.4 Hz, 2H;  $\beta$ -H), 8.90 (s, 2H; *o*-H), 8.82 (s, 2H; *o*-H), 8.43 (s, 2H; *p*-H), 8.17 (s, 2H; *p*-H), 7.71 (s, 2H; *o*-H),

–1.31 (s, 2H;  $\beta$ -H), –2.59 ppm (s, 2H; NH); MS (HRFAB):  $m/z$  (%) calcd for  $C_{36}H_{25}F_{24}N_5$ : 1223.1727  $[M]^+$ ; found: 1223.1724.

**[22]N-Pentaphyrin 3:** Purple solid (12 mg, 1%); m.p.: >300°C; UV/Vis (toluene):  $\lambda_{max}$  ( $\epsilon$ )=345 (30000), 477 (58000), 560 (61000), 1032 nm ( $4500\text{ M}^{-1}\text{ cm}^{-1}$ );  $^1\text{H NMR}$  (400 MHz,  $\text{CD}_2\text{Cl}_2$ , –50°C):  $\delta$ =9.84 (s, 1H; phenyl), 9.78 (s, 2H;  $\beta$ -H), 9.60 (d,  $J$ =5.2 Hz, 1H;  $\beta$ -H), 9.15 (d,  $J$ =5.2 Hz, 1H;  $\beta$ -H), 8.74 (m, 3H; phenyl), 8.61 (d,  $J$ =4.4 Hz, 1H;  $\beta$ -H), 8.57 (s, 3H; phenyl), 8.46 (d,  $J$ =4.4 Hz, 1H;  $\beta$ -H), 8.40 (s, 1H; phenyl), 8.39 (s, 1H; phenyl), 8.26–8.22 (m, 2H; phenyl), 8.19 (s, 1H; phenyl), 8.14 (s, 1H; phenyl), 8.04 (s, 1H; phenyl), 7.38 (s, 1H; phenyl), 2.01 (d,  $J$ =4.4 Hz, 1H;  $\beta$ -H), 1.62 (d,  $J$ =4.4 Hz, 1H;  $\beta$ -H), 1.05 (s, 1H; NH), –2.40 ppm (s, 1H;  $\beta$ -H); MS (HRFAB):  $m/z$  (%) calcd for  $C_{65}H_{25}F_{30}N_5$ : 1445.1631  $[M]^+$ ; found: 1445.1620.

**[26]Hexaphyrin 4:** Blue solid (81 mg, 7%); m.p.: >300°C; UV/Vis (toluene):  $\lambda_{max}$  ( $\epsilon$ )=328 (53000), 437 (29000), 604 (140000), 774 (8600), 854 (12000), 963 nm ( $3000\text{ M}^{-1}\text{ cm}^{-1}$ );  $^1\text{H NMR}$  (270 MHz,  $\text{CD}_2\text{Cl}_2$ , –50°C):  $\delta$ =8.62 (s, 4H;  $o$ -H), 8.23 (s, 4H;  $\beta$ -H), 8.16 (s, 4H;  $o$ -H), 8.14 (d,  $J$ =4.6 Hz, 4H;  $\beta$ -H), 7.81 (d,  $J$ =1.6 Hz, 4H;  $p$ -H), 7.49 (d,  $J$ =4.6 Hz, 4H;  $\beta$ -H), 7.25 (brs, 2H; NH), 6.06 (s, 2H;  $p$ -H), 5.50 ppm (s, 4H;  $o$ -H); MS (HRFAB):  $m/z$  (%) calcd for  $C_{78}H_{32}F_{36}N_6$ : 1736.2114  $[M]^+$ ; found: 1736.2121.

**[32]Heptaphyrin 5:** Green solid (70 mg, 6%); m.p.: >300°C; UV/Vis (toluene):  $\lambda_{max}$  ( $\epsilon$ )=407 (63000), 486 (28000), 628 (59000), 672 nm ( $69000\text{ M}^{-1}\text{ cm}^{-1}$ );  $^1\text{H NMR}$  (400 MHz,  $\text{CDCl}_3$ , 25°C):  $\delta$ =16.81 (s, 2H; NH), 11.76 (s, 2H; NH), 10.57 (s, 2H;  $\beta$ -H), 8.96 (s, 2H;  $\beta$ -H), 8.57 (s, 4H; phenyl), 8.26 (s, 2H; phenyl), 7.98 (s, 1H; phenyl), 7.94 (s, 2H; phenyl), 7.79 (s, 4H; phenyl), 7.67 (s, 3H; phenyl), 7.62 (s, 3H; phenyl), 7.39 (s, 2H; phenyl), 7.09 (d,  $J$ =4.4 Hz, 2H;  $\beta$ -H), 6.79 (s, 2H;  $\beta$ -H), 6.09 (br s, 2H;  $\beta$ -H), 5.71 (brs, 2H;  $\beta$ -H), 5.62 ppm (brs, 2H;  $\beta$ -H); MS (HRFAB):  $m/z$  (%) calcd for  $C_{91}H_{39}F_{42}N_7$ : 2027.2596  $[M]^+$ ; found: 2027.2602.

## Acknowledgements

This work was supported by Grant-in-Aids (No. 19350068 to H.I.) and World Premier International Research Center Initiative (WPI Initiative), MEXT, Japan. S.K. is grateful for a JSPS fellowship for young scientists. We thank Eiji Kinoshita and his co-workers in Shimadzu Co. Ltd., for measurements of NIR photoluminescence. N.T. and H.L. thank the Academy of Finland for the financial support.

- [1] *The Porphyrin Handbook* (Eds.: K. M. Kadish, K. Smith, R. Guillard), Academic Press, San Diego, CA, **2000**.
- [2] *Electron Transfer in Chemistry* (Ed.: V. Balzani), Wiley-VCH, Weinheim, **2001**.
- [3] a) D. Dolphin, T. G. Traylor, L. Y. Xie, *Acc. Chem. Res.* **1997**, *30*, 251–259; b) A. M. d. R. Gonsalves, A. Serra, *J. Porphyrins Phthalocyanines* **2000**, *4*, 599–604; c) K. T. Moore, I. T. Horvath, M. J. Therien, *Inorg. Chem.* **2000**, *39*, 3125–3139.
- [4] S. G. Dimagno, P. H. Dussault, J. A. Schultz, *J. Am. Chem. Soc.* **1996**, *118*, 5312–5313.
- [5] a) S. J. Lee, J. T. Hupp, *Coord. Chem. Rev.* **2006**, *250*, 1710–1723; b) K. E. Splan, C. L. Stern, J. T. Hupp, *Inorg. Chim. Acta* **2004**, *357*, 4005–4014.
- [6] J. P. Strachan, S. Gentemann, J. Seth, W. A. Kalsbeck, J. S. Lindsey, D. Holten, D. F. Bocian, *J. Am. Chem. Soc.* **1997**, *119*, 11191–11201.
- [7] a) F. A. Walker, E. Hui, J. M. Walker, *J. Am. Chem. Soc.* **1975**, *97*, 2390–2397; b) K. M. Kadish, M. Morrison, *J. Am. Chem. Soc.* **1976**, *98*, 3326–3328.
- [8] a) M. Homma, K. Aoyagi, Y. Aoyama, H. Ogoshi, *Tetrahedron Lett.* **1983**, *24*, 4343–4346; b) H. Onda, H. Toi, Y. Aoyama, H. Ogoshi, *Tetrahedron Lett.* **1985**, *26*, 4221–4224.
- [9] a) S. G. Dimagno, R. A. Williams, M. J. Therien, *J. Org. Chem.* **1994**, *59*, 6943–6948; b) E. K. Woller, S. G. Dimagno, *J. Org. Chem.* **1997**, *62*, 1588–1593; c) J. G. Goll, K. T. Moore, A. Ghosh, M. J. Therien, *J. Am. Chem. Soc.* **1996**, *118*, 8344–8354; d) K. T. Moore, J. T. Fletcher, M. J. Therien, *J. Am. Chem. Soc.* **1999**, *121*, 5196–5209.
- [10] a) Y. Terazono, D. Dolphin, *J. Org. Chem.* **2003**, *68*, 1892–1900; b) L.-M. Jin, Z. Zeng, C.-C. Guo, Q.-Y. Chen, *J. Org. Chem.* **2003**, *68*, 3912–3917; c) L.-M. Jin, L. Chen, J.-J. Yin, C.-C. Guo, Q.-Y. Chen, *J. Fluorine Chem.* **2005**, *126*, 1321–1326.
- [11] A. Ghosh, *Angew. Chem.* **2004**, *116*, 1952–1965; *Angew. Chem. Int. Ed.* **2004**, *43*, 1918–1931.
- [12] a) S. Shimizu, A. Osuka, *J. Porphyrins Phthalocyanines* **2004**, *8*, 175–181; b) S. Shimizu, A. Osuka, *Eur. J. Inorg. Chem.* **2006**, 1319–1335; c) S. Shimizu, N. Aratani, A. Osuka, *Chem. Eur. J.* **2006**, *12*, 4909–4918.
- [13] a) J. L. Sessler, D. Seidel, *Angew. Chem.* **2003**, *115*, 5292–5333; *Angew. Chem. Int. Ed.* **2003**, *42*, 5134–5175; b) J. L. Sessler, E. Tomat, *Acc. Chem. Res.* **2007**, *40*, 371–379.
- [14] a) H. Furuta, H. Maeda, A. Osuka, *Chem. Commun.* **2002**, 1795–1804; b) A. Srinivasan, H. Furuta, *Acc. Chem. Res.* **2005**, *38*, 10–20.
- [15] A. Jasat, D. Dolphin, *Chem. Rev.* **1997**, *97*, 2267–2234.
- [16] a) T. K. Chandrashekar, S. Venkatraman, *Acc. Chem. Res.* **2003**, *36*, 676–691; b) R. Misra, T. K. Chandrashekar, *Acc. Chem. Res.* **2008**, *41*, 265–279.
- [17] a) A. Krivokapic, A. R. Cowley, H. L. Anderson, *J. Org. Chem.* **2003**, *68*, 1089–1096; b) A. Krivokapic, H. L. Anderson, *Org. Biomol. Chem.* **2003**, *1*, 3639–3641.
- [18] a) M. Suzuki, A. Osuka, *Org. Lett.* **2003**, *5*, 3943–3946; b) S. Shimizu, N. Aratani, A. Osuka, *Chem. Eur. J.* **2006**, *12*, 4909–4918; c) R. Taniguchi, S. Shimizu, M. Suzuki, J. Shin, H. Furuta, A. Osuka, *Tetrahedron Lett.* **2003**, *44*, 2505–2507.
- [19] W. Maes, J. Vanderhaeghen, W. Dehaen, *Chem. Commun.* **2005**, 2612–2614.
- [20] a) J. L. Sessler, T. D. Mody, V. Lynch, *J. Am. Chem. Soc.* **1993**, *115*, 3346–3347; b) H. Furuta, T. Asano, T. Ogawa, *J. Am. Chem. Soc.* **1994**, *116*, 767–768.
- [21] P. Corbett, J. Leclaire, L. Vial, K. R. West, J.-L. Wietor, J. K. M. Sanders, S. Otto, *Chem. Rev.* **2006**, *106*, 3652–3711.
- [22] a) P. J. Chmielewski, L. Latos-Grażyński, K. Rachlewicz, *Chem. Eur. J.* **1995**, *1*, 68–73; b) K. Rachlewicz, N. Sprutta, L. Latos-Grażyński, P. J. Chmielewski, L. Szterenberg, *J. Chem. Soc. Perkin Trans. 2* **1998**, 959–967.
- [23] 24 $\pi$ -electron *N*-fused pentaphyrin is well known in the literature,<sup>[24]</sup> however it was not obtained in this reaction.
- [24] a) J.-Y. Shin, H. Furuta, A. Osuka, *Angew. Chem.* **2001**, *113*, 639–641; *Angew. Chem. Int. Ed.* **2001**, *40*, 619–621; b) S. Mori, J.-Y. Shin, S. Shimizu, F. Ishikawa, H. Furuta, A. Osuka, *Chem. Eur. J.* **2005**, *11*, 2417–2425.
- [25] a) M. G. P. M. S. Neves, R. M. Martins, A. C. Tomé, A. J. D. Silvestre, A. M. S. Silva, V. Félix, M. G. B. Drew, J. A. S. Cavaleiro, *Chem. Commun.* **1999**, 385–386; b) T. K. Ahn, J. H. Kwon, D. Y. Kim, D. W. Cho, D. H. Jeong, S. K. Kim, M. Suzuki, S. Shimizu, A. Osuka, D. Kim, *J. Am. Chem. Soc.* **2005**, *127*, 12856–12861.
- [26] M. Suzuki, A. Osuka, *Chem. Eur. J.* **2007**, *13*, 196–202.
- [27] a) H. S. Rzepa, *Chem. Rev.* **2005**, *105*, 3697–3715; b) R. Herges, *Chem. Rev.* **2006**, *106*, 4820–4842; c) M. Stepień, L. Latos-Grażyński, N. Sprutta, P. Chwalisz, L. Szterenberg, *Angew. Chem.* **2007**, *119*, 8015–8019; *Angew. Chem. Int. Ed.* **2007**, *46*, 7869–7873.
- [28] Y. Tanaka, S. Saito, S. Mori, N. Aratani, H. Shinokubo, N. Shibata, Y. Higuchi, Z. S. Yoon, K. S. Kim, S. B. Noh, J. K. Park, D. Kim, A. Osuka, *Angew. Chem.* **2008**, *120*, 693–696; *Angew. Chem. Int. Ed.* **2008**, *47*, 681–684.
- [29] a) S. Saito, A. Osuka, *Chem. Eur. J.* **2006**, *12*, 9095–9102; b) S. Shimizu, J.-Y. Shin, H. Furuta, R. Ismael, A. Osuka, *Angew. Chem.* **2003**, *115*, 82–86; *Angew. Chem. Int. Ed.* **2003**, *42*, 78–82.
- [30] The absorption spectral changes in the protonation of sapphyrin **2** on successive additions of TFA were measured in  $\text{CH}_2\text{Cl}_2$  (Figure S5 in the Supporting Information). On successive additions of TFA (0–100 equiv) new absorption arising from the protonated **2**, which is accompanied by three isosbestic points at 490 nm, 670 nm, and 722 nm, emerges gradually, whereas absorption arising from the neutral **2** disappears concomitantly.

- [31] P. J. Spellane, M. Gouterman, A. Antipas, S. Kim, Y. C. Liu, *Inorg. Chem.* **1980**, *19*, 386–391.
- [32] J. H. Wilford, M. D. Archer, J. R. Bolton, T. F. Ho, J. A. Schmidt, A. C. Weedon, *J. Phys. Chem.* **1985**, *89*, 5395–5398.
- [33] M. Shinoya, H. Furuta, V. Lynch, A. Harriman, J. L. Sessler, *J. Am. Chem. Soc.* **1992**, *114*, 5714–5722.
- [34] N. V. Tkachenko, L. Rantala, A. Y. Tauber, J. Helaja, P. H. Hynninen, H. Lemmetyinen, *J. Am. Chem. Soc.* **1999**, *121*, 9378–9387.
- [35] G. A. Baker, F. V. Bright, M. R. Detty, S. Pandey, C. E. Stilts, H. Yao, *J. Porphyrins Phthalocyanines* **2000**, *4*, 669–683.

Received: June 5, 2008

Revised: August 8, 2008

Published online: October 21, 2008